Avrupa Bilim ve Teknoloji Dergisi
Sayı 27, S. 471-478, Kasım 2021

Araştırma Makalesi

www.ejosat.com ISSN:2148-2683

European Journal of Science and Technology
No. 27, pp. 471-478, November 2021

Research Article

Validation of an elastomeric bearing characterized with finite element hyperelastic models

Faisal Ahmed[1*], Fatih Alemdar[2]

[1*] Yildiz Technical University, Faculty of Engineering, Department of Construction, İstanbul, Turkey, (ORCID: 0000-0002-1799-2558), faisalalneela@gmail.com
[2] Yildiz Technical University, Faculty of Engineering, Department of Construction, İstanbul, Turkey, (ORCID: 0000-0002-8752-0310), falemdar@yildiz.edu.tr

(First received 1 May 2021 and in final form 6 September 2021)

(**DOI:** 10.31590/ejosat.930964)

ATIF/REFERENCE: Ahmed, F. & Alemdar, F. (2021). Validation of an elastomeric bearing characterized with finite element hyperelastic models. *European Journal of Science and Technology*, (27), 471-478.

Abstract

Elastomeric bearing is a crucial element of a structure. To study these elements' behavior under different loads, a correct strain energy function should be selected to predict the nonlinear hyperelastic behavior accurately. Physical compression test performed on a sample of a steel laminated elastomeric bearing, which is originally used on structure foundation to resist seismic forces. A finite element software was used to simulate physical test for seven different hyperelastic models. Error percentages were also calculated and compared between all models with the experimental data. The results of these seven models were validated in order to select the most fitted form. Multiple models gave an accurate prediction of this element behavior. Reduced Polynomial form was the best choice to model compression tests and the finite element simulation showed an accurate prediction for bearing behavior, the model curve is perfectly fitted with the physical test curve and the maximum error percentage was less than 7% and less than 2% minimum error.

Keywords: Elastomeric bearing, Hyperelastic material, Finite element model, Reduced polynomial, Neo-Hooke

Sonlu eleman hiperelastik modellerle karakterize edilen bir elastomerik mesnedin doğrulanması

Öz

Elastomerik mesnet, bir yapının çok önemli bir unsurudur. Bu elemanların farklı yükler altındaki davranışını incelemek için, doğrusal olmayan hiperelastik modeli doğru bir şekilde tahmin etmek için doğru bir gerinim enerjisi fonksiyonu seçilmelidir. Sismik kuvvetlere karşı bina temellerinde kullanılan çelik tabakalarla güçlendirilmiş bir elastomerik mesnet numunesi üzerinde gerçekleştirilen fiziksel basınç testi yapıldı. Fiziksel testleri simüle etmek için bir sonlu eleman yazılımı kullanılmıştır. Hata yüzdesi hesaplandı ve test verisiyle yedi model arasında karşılaştırma yapıldı. Bu yedi modelin sonuçları, en uygun formu seçmek için doğrulanmıştır. Birden çok model, bu eleman davranışının doğru bir tahminini verdi. Azaltılmış Polinom formu ise basınç testlerini modellemek için en iyi seçimdi ve sonlu elemanlar simülasyonu, eğri uydurma ve hata yüzdesi bakımından eğilme davranışı için doğru bir tahmin gösterdi.

Anahtar Kelimeler: Elastomerik mesnet, Hyperelastic malzeme , Sonlu eleman modeli.

[*] Corresponding Author: faisalalneela@gmail.com

1. Introduction

Bearings are elastomeric material reinforced with steel layers; these layers' distributions and thickness depend on the use of the element (**Hata! Başvuru kaynağı bulunamadı.**). The bearing is an element that translates stresses between structure elements while allowing an absolute degree of freedom (Fragnet, 2013). A bridge bearing is usually the element that connects the deck with supports (Fragnet, 2013). Bearings are also used in structure foundations to carry the vertical loads without damaging the structure, especially considering the eccentricity that could occur during the earthquake movements. A large proportion of the world's population dwells in seismically hazardous zones and suffers from earthquakes of varying magnitude (EKŞİ, 2019). These earthquakes cause huge damage to properties and life loss for years. Therefore, bearings are used to reduce horizontal seismic force by using the advantages of the hyperelastic properties.

Figure 1 An elastomeric bearing

Hyperelastic material such as elastomers is a widely used material in various industries, and it has multiple applications (Shahzad et al., 2015). The main mechanical feature of the elastomer family is the extraordinary elasticity. When a load is applied on an elastomer, it can experience significant elongation from its original length and get back to the initial shape after the load is removed. Therefore, elastomers consider as unique materials in civil engineering. The behavior of the elastomeric material is highly nonlinear, and a simple modulus of elasticity that can be predicted from the stress-strain curve is no longer sufficient. Therefore, it is essential to characterize this material to understand its behavior.

This study aims to define and choose the most accurate hyperelastic material model then use it to model a reinforced elastomeric bearing. The most precise model should be able to predict the behavior of this material under different loading conditions. To achieve the objective of this study, ABAQUS CAE 2017 software was used for FE modeling, and then comparison and validation were made between the model results and physical tests.

2. Background

Turkey is located at one of the most active earthquake zones called Mediterranean-Alpine-Himalayan. Between 1900 and 2005, the number of earthquakes between the magnitudes 5-5.9 is 1170, 6-6.9 is 155, and 7-8 is 34 (EKŞİ, 2019) (AFAD, 2019). These earthquakes have caused significant loss of life and great damage to human-made structures. Therefore, the concept of seismic isolation began to gain prominence, especially after the 1999 Marmara Earthquake (EKŞİ, 2019). Hyperelastic materials are one of the materials used in these isolation systems to resist seismic forces. Characterization is required to understand the nonlinear behavior of this material.

Abaqus has two main types of models in terms of defining the strain energy function. The first group of models depends on the phenomenological hypothesis, which solves the problem from the aspect of continuum mechanics (Tobajas et al., 2018) (Shahzad et al., 2015). The other type of solution depends on the microscopic structure to characterize the behavior, the material reaction is considered from the aspect of microstructure (Arruda et al., 1993) (Abaqus, 2012). All hyperelastic models share the same input requirements (Abaqus-Docs, 2017), these input data can be evaluated by testing the rubber in a different mode. The appropriate experiments to define a hyperelastic material are not yet clearly defined by national or international standards organizations (Miler, 2004). This difficulty derives from the complicated mathematical models required to represent both the nonlinear and nearly incompressible elastomers' properties (Miler, 2004). Therefore, the evolution of using this material required trial and error rather than basic equations.

2.1. The Required Tests

Defining hyperelastic material in FE usually required testing rubber in different modes. FE software documentation gave recommendations for the appropriate way to perform the required tests to get better input data (Abaqus-Docs, 2017). Four types of deformation modes are required to define this material:

2.1.1. Uniaxial tension and compression

The uniaxial test is done by stretching or compress a specimen from two sides. However, pure compression is generally hard to achieve because of the friction between specimen and the test device.

2.1.2. Biaxial tension and compression

An equal tensile force is applied to all specimen sides. The biaxial machine is not commonly available due to high prices and low uses. Therefore, several researchers developed custom fixtures to use a uniaxial test machine in performing this test (Barroso et al., 2012) (Medellín et al., 2017) (Crocker et al., 1999).

2.1.3. Planar tension (also known as pure shear)

To achieve pure shear, the stretching should also be from the wider two sides; the specimen should have more width than the height. In fact, the width should be at least ten times more than the height of the specimen (Miler, 2004).

2.1.4. Volumetric compression

A volumetric test is used to evaluate bulk modulus and compressibility. Force is applied to a fully confined specimen to measure Bulk modulus, which is usually 2-3 greater than the shear modulus (Miler, 2004).

Figure 2 shows more details about the required tests. For ideal incompressible hyperelastic material, the following test modes have become identical: uniaxial tension with biaxial compression, uniaxial compression with biaxial tension, and planar tension with planar compression. With these corresponding test modes, only three independent deformations are required to be evaluated. Therefore, most of the available researches depends on

the tension mode of these tests except for volumetric. The combination of these four tests data can give a good characterization of the hyperelastic material behavior.

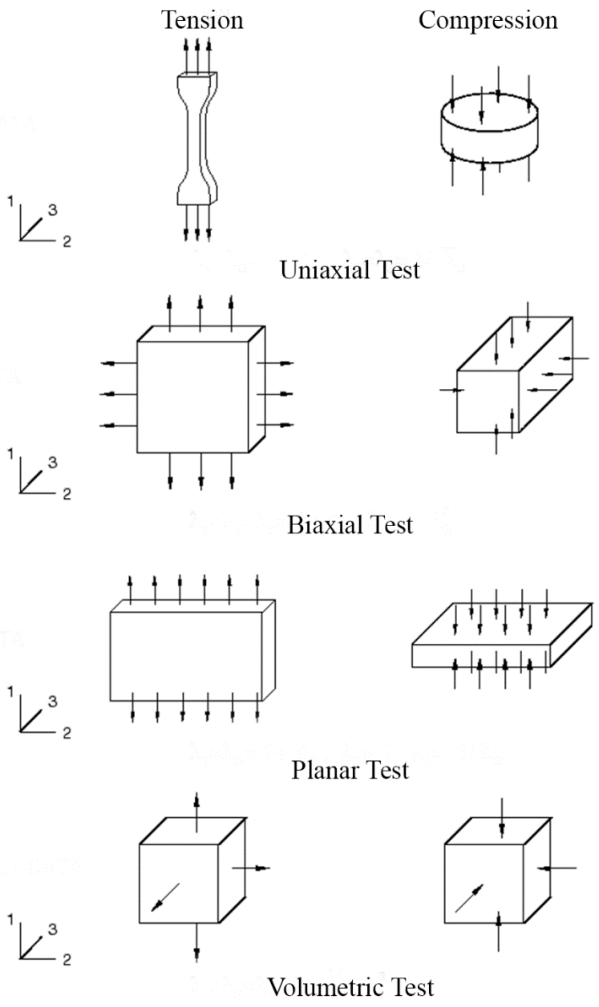

Figure 2 The required tests to define a hyperelastic material (Abaqus-Docs, 2017)

Several studies for defining hyperelastic models are available, and each research has a different material and test setup. Therefore results vary between researchers. Most of these studies only defined the hyperelastic model without an application on elastomeric elements. In the next section, several hyperelastic definition tests and applications will be reviewed.

3. Compression Test

A compression test was made on a sample of elastomeric bearing. An elastomeric bearing sample cut from the original bearing. The sample's dimensions are 100 mm by 100 mm with a total thickness of 62 mm. It consists of three natural rubber elastomeric layers and four steel layers. The thicknesses of the rubber and the steel parts are 42 mm and 20 mm, respectively. Instron 8803 Fatigue Testing System was used to perform this experiment. This system has a 500 kN static and dynamic load capacity. This feature allows us to apply dynamic forces properly on the specimen under a specific frequency. The compression load is executed to this sample until the structural failure occurs. As expected for a hyperelastic material, a nonlinear stress-strain curve was obtained. The stiffness was also increased as the compression load increased since the bearing may suffer structural damages under high strain levels. Therefore, high stiffness elastomeric material is required in this type of element.

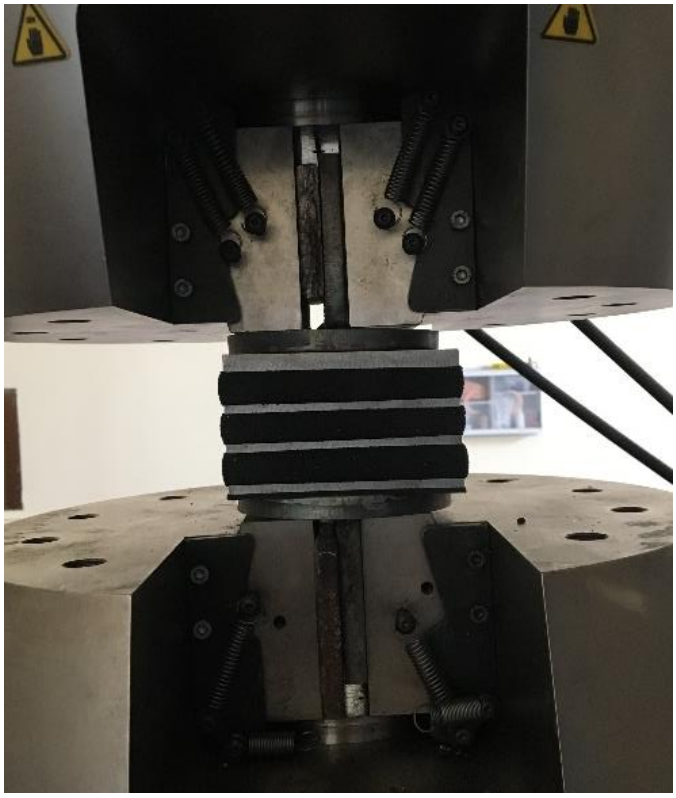

Figure 3 Specimen through testing

shows the specimen in the test machine.

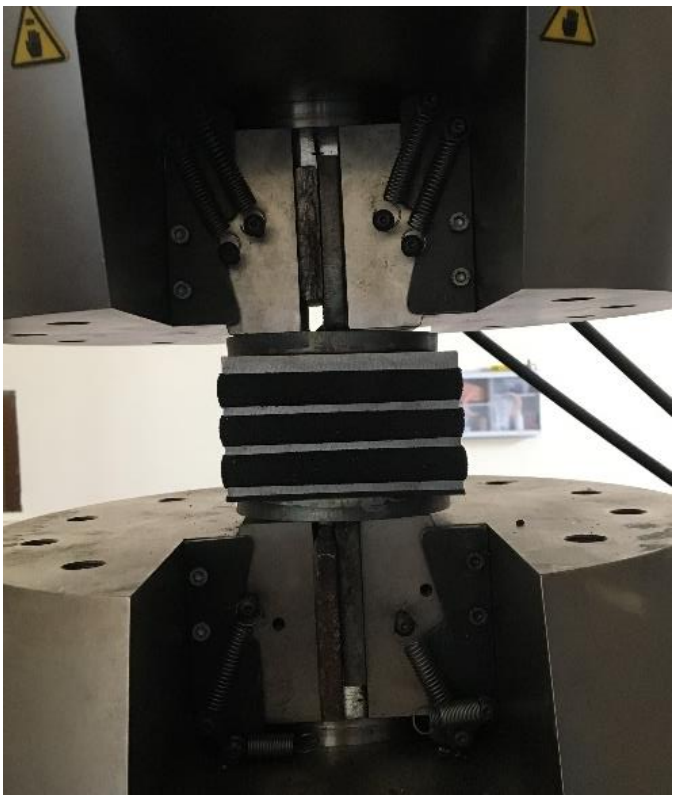

Figure 3 Specimen through testing (EKŞİ, 2019)

After 36 percent of strain or 15.12 mm shortening from the total 42 mm rubber thickness at a stress of 22 MPa, bonding failure between the elastomer layers and steel parts started to

appear in the tension area. As expected from the hyperelastic behavior of the elastomer material layers, the nonlinear stress-strain graph is obtained as shown in Figure 4.

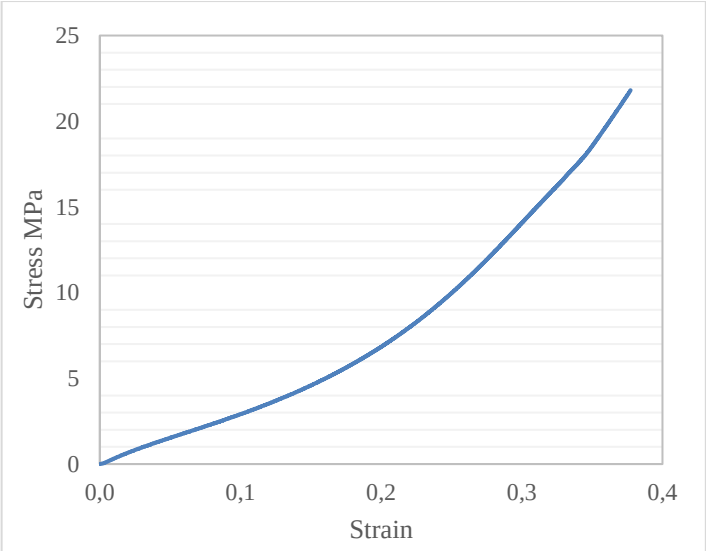

Figure 4 Stress-Strain curve for bearing specimen

4. Finite Element Hyperelastic Modeling

ABAQUS CAE 2017 software was used in the modeling process (Abaqus-Docs, 2017). (Sugihardjo et al., 2018) tested a similar material for all four required tests to define a hyperelastic material. Therefore, test results of the study (Sugihardjo et al., 2018) were used as an input to evaluate ABAQUS hyperelastic material.

Finite element validation aims to find the best model to define this material and fit the experimental results. After finding the most suitable model, the other behaviors of this structural element can be predicted. There is several finite element software that can solve and model a hyperelastic material. ABAQUS software is one of the best programs that can be used in FE modeling. All of the hyperelastic models used to define strain energy function (SEF) to characterize the material behavior are pre-defined in the software. These hyperelastic models mostly share the exact input requirements. As discussed before, these inputs should be obtained from the stress-strain data taken from stretching the elastomer in different modes. Hyperelastic models have been classified according to their main family as shown below.

- Arruda-Boyce
- Mooney-Rivlin (Polynomial N1)
- Ogden:
    - First-order N1
    - Second-order N2
- Reduced Polynomial:
    - Neo Hooke (first-order N1)
    - Second-order N2
    - Yeoh (third-order N3)

To evaluate hyperelastic material in Abaqus new material should be created, this material will be used generally to evaluated all models. In the mechanical properties, hyperelastic material should be selected. After this property is selected, the used test data will be added for each test type, four tests available as discussed before. Abaqus also gives the ability to apply smoothing points to test data, experimental tests can contain some noise in results data which can affect the quality of the strain energy derived function. The final step will be evaluating all models, from material then evaluate choice, specific tests data can be selected in the evaluation process. Minimum and maximum strain values should be set for each test, the best value is to add physical experiments strain values in order to get the best fitting curves. Abaqus also gives the ability to simulate simple shear test to compare it with the experimental result if there is any. Ogden model accepts only one of the three shear tests besides the volumetric test.

After finishing all settings the software will evaluate all models coefficients for every model, also it will give information for each test and if the model is stable to use in model simulation. The resulted coefficients from this evaluation process are taken and used to define the hyperelastic material for the elastomeric bearing model, more details about each model will be presented in the modeling and validation section.

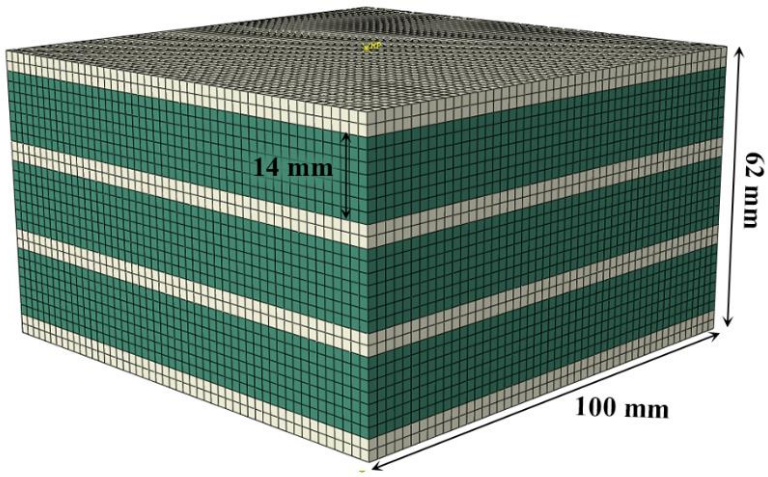

Figure 5 3D Model for the spacimen

4.1. Model Setup

The exact dimensions for experimental specimen have been modeled and coefficients evaluated before defining it in the material property. All parts have been linked together in a single instance for better performance analysis. **Hata! Başvuru kaynağı bulunamadı.** represents the three-dimensional view of the specimen.

4.1.1. Mesh Size

After several analyses using different mesh sizes, 2 mm mesh size was used in the simulation process. This small mesh size can lead to longer analysis time, however; it gives more accurate results. The total number of elements is 72500 and the elements are distributed as shown in **Hata! Başvuru kaynağı bulunamadı.**.

4.1.2. Boundary conditions

The boundary conditions were defined to simulate the physical test environment which undergoes pure compression. Constraints are added to the base of the bearing in the initial step to prevent the movement in any direction (U1 = U2 = U3 = UR1 = UR2 = UR3 = 0). Vertical displacement of 15.12 mm are applied to the top surface of the specimen to simulate the physical experiment, while the displacement in other directions was restricted (U2 = -15.12, U1 = U3 = UR1 = UR2 = UR3 = 0).

Force-displacement and stress-strain results were recorded at the top surface to compare with the test results. Figure shows the loading steps in the FE model simulation. After finishing all the required setup, the model has been run for all seven different material models. Output history data has been observed similar to the physical test.

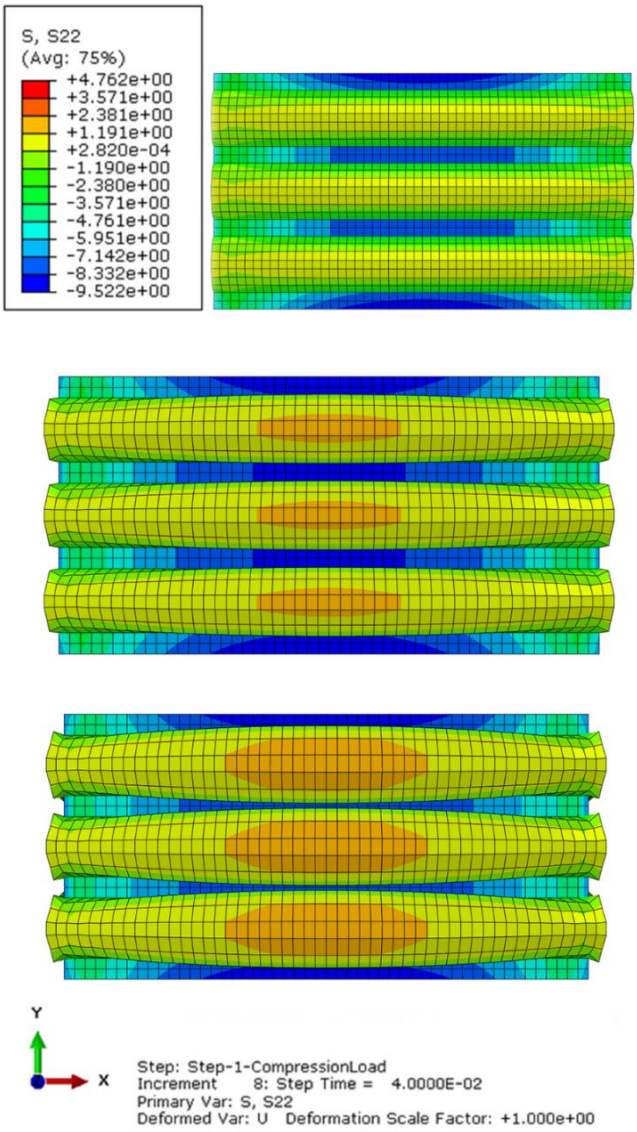

Figure 6 Loading steps applied to the FE model

4.2. Modeling and Validation

Test simulations made with hyperelastic models and models have been arranged into four groups and seven models according to their primary forms. To comparison all these models with test results, error percentages were calculated using the following equation.

$$\%Error = \frac{Test\ Results - Finite\ Element\ Results}{Test\ Results} * 100 \quad Eq.\ 1$$

4.2.1. Arruda-Boyce

The first model selected in this research depends on three parameters which are μ, λ_m and D, as shown in $U = \mu\left[\frac{1}{2}(\bar{I}_1 - 3) + \frac{1}{20\lambda_m^2}(\bar{I}_1^2 - 9) + + \frac{1}{1050\lambda_m^4}(\bar{I}_1^3 - 27)\right] + \frac{1}{D}\left(\frac{J_{e\ell}^2 - 1}{2} - lnJ_{e\ell}\right)$, Eq. 2. These parameter values were calculated as shown in Table 1:

$$U = \mu\left[\frac{1}{2}(\bar{I}_1 - 3) + \frac{1}{20\lambda_m^2}(\bar{I}_1^2 - 9) + + \frac{1}{1050\lambda_m^4}(\bar{I}_1^3 - 27)\right] + \frac{1}{D}\left(\frac{J_{e\ell}^2 - 1}{2} - lnJ_{e\ell}\right), \quad Eq.\ 2$$

U is the strain energy per unit volume;
μ, λ_m and D: Temperature-dependent material parameters,
$\bar{I}_1$: The first deviatoric strain invariant

Table 1 Arruda-Boyce coefficients

μ	0.36795
λ_m	2.3191
D	0.00065

After the analysis was run, the stress-stress strain curve for the bearing material was drawn as shown in Figure . The results of the test and the model were compared and a significant difference was noticed in the behavior of the stress-strain curve.

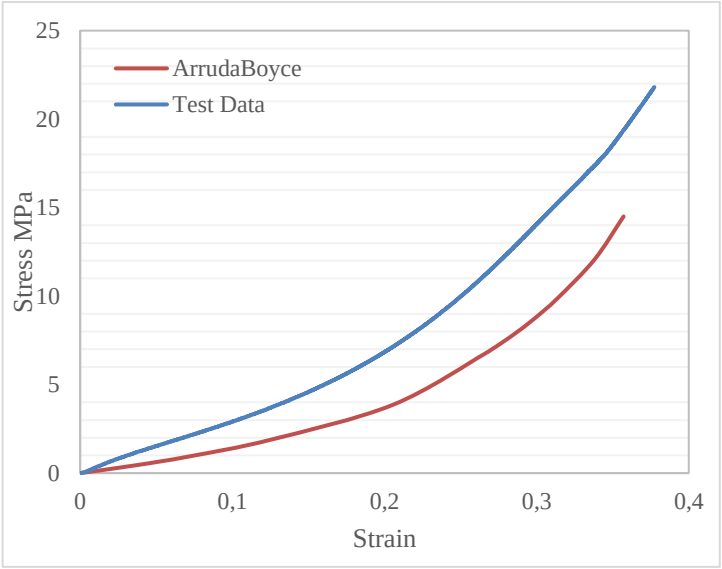

Figure 7 Stress-Strain curves for Arruda Boyce hyperelastic model.

Error percent is up to 55% at maximum when the strain is 0.9, while the lowest error was 24% at its maximum strain. This error range can be considered as high.

4.2.3. Mooney-Rivlin (Polynomial)

Moony Rivlin model belongs to the polynomial form which is first introduced by the two scientists Mooney and Rivlin (Tobajas et al., 2018), as shown in $U = C_{10}(\bar{I}_1 - 3) + C_{01}(\bar{I}_2 - 3) + \frac{1}{D_1}(J^{e\ell} - 1)^2$, Eq. 3. Stress-strain curves were obtained with the same process, coefficients used in the material property were shown in **Hata! Başvuru kaynağı bulunamadı.**. Results are compared in **Hata! Başvuru kaynağı bulunamadı.**. A high error percent was indicated, which was up to 50% at the maximum load.

$$U = C_{10}(\bar{I}_1 - 3) + C_{01}(\bar{I}_2 - 3) + \frac{1}{D_1}(J^{el} - 1)^2, \quad Eq.\ 3$$

U is the strain energy per unit volume;
$C_{10}, C_{01}\ and\ D_1$: Temperature-dependent material parameters;
$\bar{I}_1$: The first deviatoric strain invariant

Table 2 Mooney-Rivlin coefficients

C10	0.18186
C01	0.036242
D1	0.000645

The analysis was defined with orders from first to third (Neo-Hooke N1, N2, Yeoh N3), Yeoh form is third-order reduced polynomial form first introduced by (Yeoh, 1993). General form is presented in $U = \sum_{i=1}^{N} C_{i0}(\bar{I}_1 - 3)^i + \sum_{i=1}^{N} \frac{1}{D_1}(J^{el} - 1)^{2i}$, Eq. 4, parameters for all orders were obtained from FE solutions as listed in **Hata! Başvuru kaynağı bulunamadı.**. Results from stress-strain show a very close behavior to the physical test data, as shown in Figure . Neo-Hooke and N2 models show a very close prediction with an error of less than 10%, while Yeoh's error rises to a higher level as shown in **Hata! Başvuru kaynağı bulunamadı.**.

Table 3 Coefficients for Reduced Polynomial models

Neo-Hooke N1	
C10	0.54092
D1	0.00064512
Reduced Polynomial N2	
C10	0.406947
C20	0.007435
D1	0.000664
D2	0.0000643
Yeoh N3	
C10	0.21777
C20	-0.004460
C30	0.002040
D1	0.000689
D2	0.0000656
D3	0.00000065

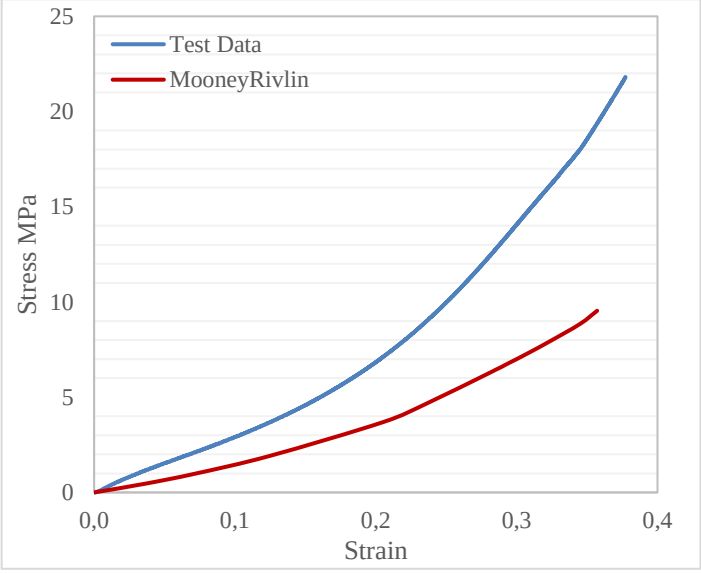

Figure 8 Stress-Strain curves for polynomial models

The first-order result gave a massive error percent, up to 69%, making it the highest error in the whole series of experiments. In comparison, the second-order gave better results and closer to the physical specimen. The analysis shows less than 17% error, making it more acceptable.

4.2.2. Reduced Polynomial

$$U = \sum_{i=1}^{N} C_{i0}(\bar{I}_1 - 3)^i + \sum_{i=1}^{N} \frac{1}{D_1}(J^{el} - 1)^{2i}, \quad Eq.\ 4$$

U is the strain energy per unit volume;
N is a material parameter;
$C_{i0}\ and\ D_i$: are temperature dependent material parameters.
$\bar{I}_1$ are the first deviatoric strain invariants.

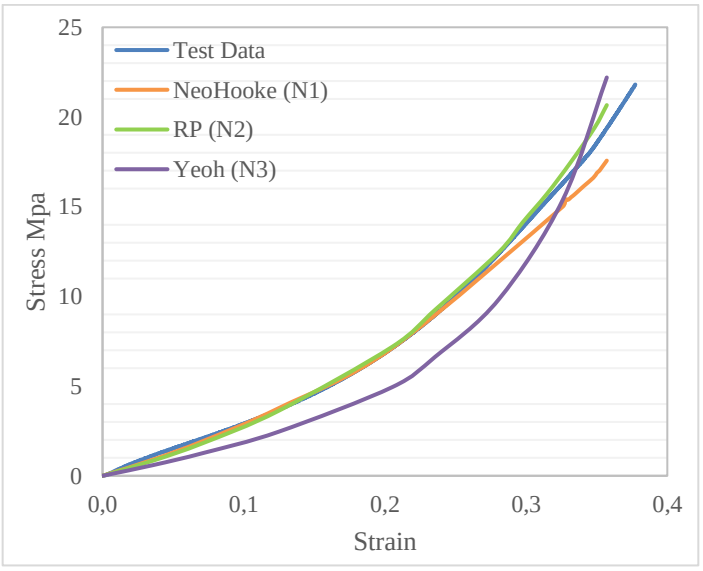

Figure 9 Stress-Strain curves for Reduced polynomial models

4.2.4 Ogden

Ogden was the final form used in this study. The model is shown in $U = \sum_{i=1}^{N} \frac{2\mu_i}{\alpha_i^2}\left(\overline{\lambda}_1^{\alpha_i} + \overline{\lambda}_2^{\alpha_i} + \overline{\lambda}_3^{\alpha_i} - 3\right) + \sum_{i=1}^{N} \frac{1}{D_1}\left(J^{e\ell} - 1\right)^{2i}$, Eq. 5, it was first proposed in 1972 by (Ogden, 1972). Two different analyses were described for the first (N1) and second (N2) orders in **Hata! Başvuru kaynağı bulunamadı.**. Results for stress-strain data are shown in **Hata! Başvuru kaynağı bulunamadı.**.

$$U = \sum_{i=1}^{N} \frac{2\mu_i}{\alpha_i^2}\left(\overline{\lambda}_1^{\alpha_i} + \overline{\lambda}_2^{\alpha_i} + \overline{\lambda}_3^{\alpha_i} - 3\right) + \sum_{i=1}^{N} \frac{1}{D_1}\left(J^{e\ell} - 1\right)^{2i}, \quad Eq.\ 5$$

U is the strain energy per unit volume;

$\overline{\lambda}_i$ are the deviatoric principal stretches, $\overline{\lambda}_i = J^{-\frac{1}{3}}\lambda_I$, $\lambda_I$are the principal stretches;

N is a material parameter;

$\mu_i, \alpha_i \; and \; D_i$: are temperature dependent material parameters.

Table 4 Coefficients for Ogden model

First-order N1	
Mu1	0.150945
Alpha1	1.645819
D1	0.000689
Second-order N2	
Mu1	0.066921
Alpha1	4.513467
Mu2	0.631607
Alpha2	-0.371077
D1	0.000689
D2	0.0000635

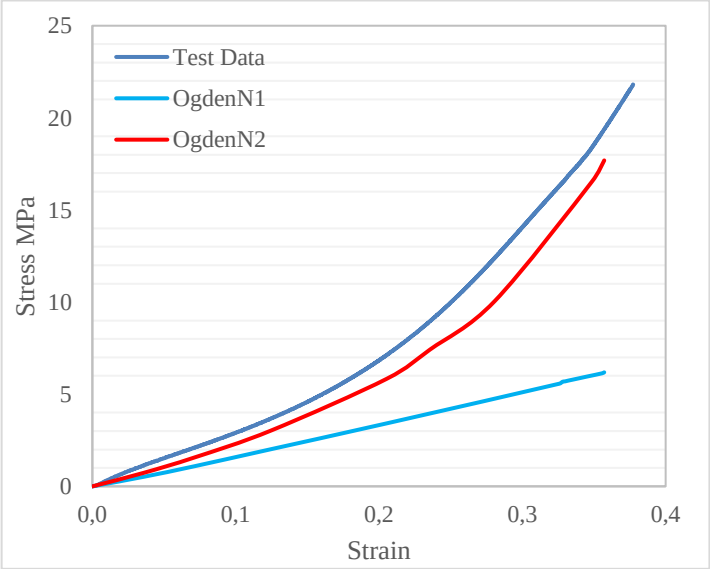

Figure 10 Stress-Strain curves for Ogden form and test data

The results of the first-order model gave a massive error. While the second-order gave better results and the curve prediction was very close to the real test.

5. Discussion

Error percentage for all model results was listed in **Hata! Başvuru kaynağı bulunamadı.** and curve fitting was used to make the final decision. Reduced Polynomial form was selected to model the material for shear tests since it has the lowest error and had the best curve fit with the experimental result. However, there is more than one model that gave acceptable results with less than 25% of error. Second-order Ogden and Neo-Hooke forms also gave good predictions, especially for Neo-Hooke which shows an error of less than 9%, but the Neo-Hooke model failed at high strain values. In terms of the Ogden model (N2), it also produced acceptable results, but the curve was not fitted perfectly with test data. First-order Ogden (N1) model gave the highest error in the whole series of analyses with a value up to 69%. Mooney-Rivlin also was not the best solution, high error percentages were obtained up to 50% at the maximum displacement.

Table 5 Maximum and minimum error for every model

Model	Min Error %	Max Error %
Arruda-Boyce	25	54
Neo-Hooke (N1)	0.33	9
Reduced Polynomial N2	1.5	7
Yeoh (N3)	6.6	30
Mooney-Rivlin	47	50
Ogden N1	40	69
Ogden N2	8	17

6. Conclusion and Recommendations

The compression test was conducted on elastomeric bearing specimen and FE simulations of this test specimen were performed. Comparisons were made between seven hyperelastic models to find the best model that can fit this rubber material. Reduced Polynomial was selected to model shear tests as it was the most fitted form. However, some observations are found from the results,

- The first-order reduced polynomial hyperelastic model (Neo-Hooke) can give a good characterization under compression loadings. There is a good correlation between test data and model results. On the other hand, stress results show little lower values in the model.
- The second best match is the reduced polynomial model. The minimum error is 1.5% and the best match was obtained for the maximum stress values.
- Some models can succeed in predicting the behavior only for small displacement values, when strain value increases the error will increase as shown in the results of Neo-Hooke and Ogden (N2) forms.
- Volumetric coefficients or the compressibility behavior are hard to predict by FE simulations. No difference can be noticed even when D coefficients were used as zero. Hyperelastic material has very small compressibility, it

can take years to detect the compressed value. Therefore, it is hard to be noticed in short simulation analysis.

- Hyperelastic models would be a glimpse of the research for future work that will match cyclic load. In order to get a perfect fitting for cyclic loads in rubbers, viscoelastic properties should be added beside the hyperelastic properties. Viscoelasticity is a time-dependent property that can be found by importing load versus time data for different modes of testing.

References

Abaqus. (2012). Analysis User's Manual 6.12, Volume II.

Abaqus-Docs. (2017). *Hyperelastic behavior of rubberlike materials.* Retrieved from Abaqus Documentaions: https://abaqus-docs.mit.edu/2017/English/SIMACAEMATRefMap/simamat-c-hyperelastic.htm

AFAD. (2019, April 10). *T.C. İÇİŞLERİ BAKANLIĞI Afet ve Acil Durum Yönetimi Başkanlığı*. Retrieved from https://deprem.afad.gov.tr/depremkatalogu

Arruda, E. M. (1993). A three-dimensional constitutive model for the large stretch behavior of rubber elastic materials. *Journal of the Mechanics and Physics of Solids, 41*(2), 389-412. Retrieved from http://dx.doi.org/10.1016/0022-5096(93)90013-6

Barroso, A. C. (2012). Biaxial testing of composites in uniaxial machines: manufacturing of a device, analysis of the specimen geometry and preliminary experimental results. *15th European Conference on Composite Materials: Composites at Venice, ECCM., 2012*.

Crocker, L. E. (1999). Hyperelastic modelling of flexible adhesives.

EKŞİ, K. (2019). *Investigate Elastomeric Bearings Under Fatigue Loading.* Master Thesis, Yildiz Technical University.

Fragnet, M. (2013). Elastomers and Rubbers used in Civil Engineering. Organic Materials for Sustainable Construction.

Medellín, L. F. (2017). Design of a biaxial test module for uniaxial testing machine. *4.8*, 7911-7920.

Miler, K. (2004). Testing elastomers for finite element analysis. *Axel Products*.

Ogden, R. W. (1972). Large deformation isotropic elasticity–on the correlation of theory and experiment for incompressible rubberlike solids. *Proceedings of the Royal Society of London. A. Mathematical and Physical Sciences, 326*(1567), 565-584. Retrieved from http://dx.doi.org/10.1098/

Shahzad, M. K. (2015). Mechanical characterization and FE modelling of a hyperelastic material. *Materials Research 18.5*, 918-924.

Sugihardjo, H. T. (2018). FE Model of Low Grade Rubber for Modeling Housing's Low-Cost Rubber Base Isolators. *Civil engineering journal*, 24-45.

Tobajas, R. e. (2018). Visco-hyperelastic model with damage for simulating cyclic thermoplastic elastomers behavior applied to an industrial component. *Polymers, 10*(6), 668.

Yeoh, O. H. (1993). Some forms of the strain energy function for rubber. *Rubber Chemistry and technology, 66*(5), 754-771.